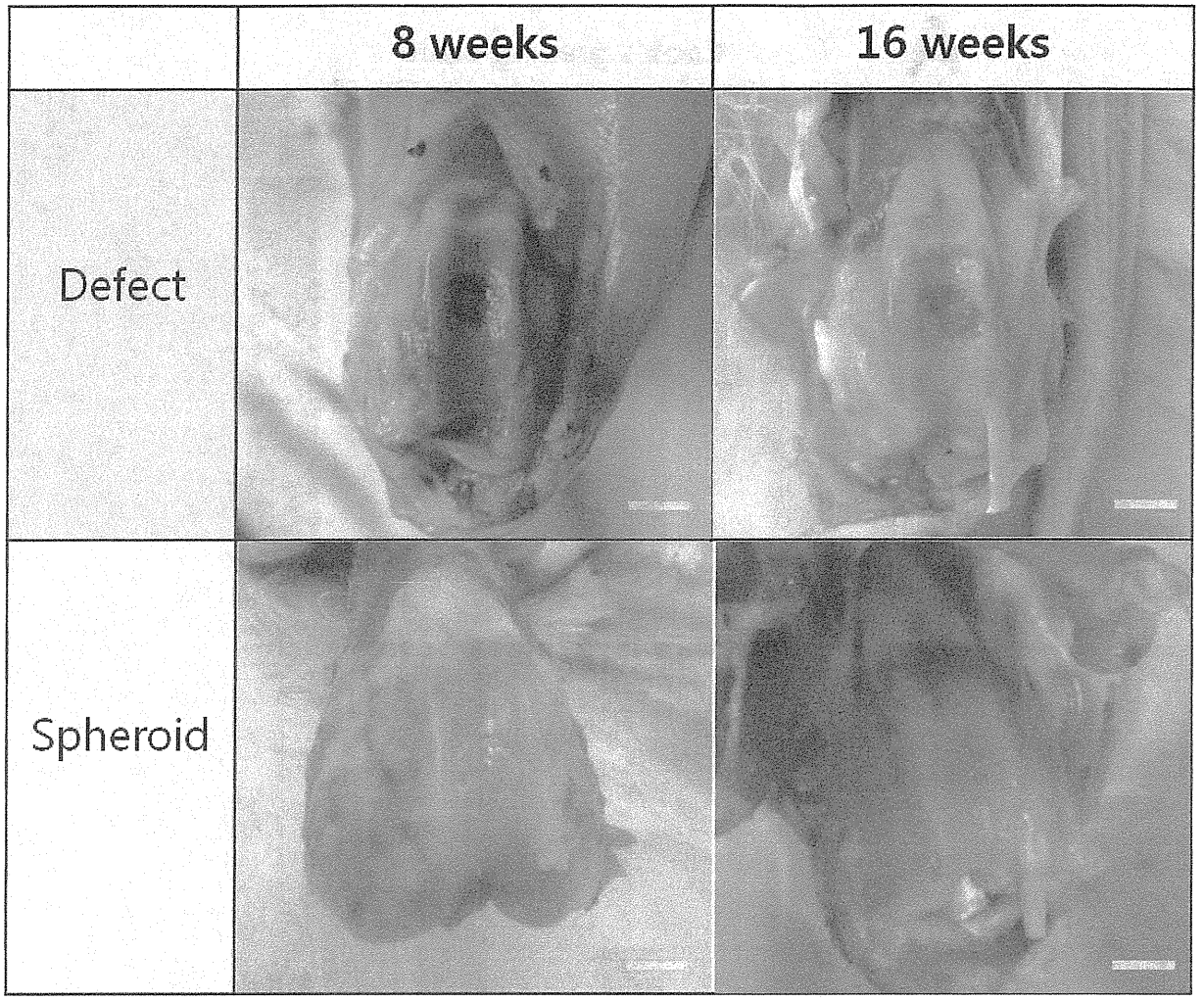


**Fig. 6.** Macroscopic analyses for the *in vivo* study. Gross observations of femoral condyles at 8 and 16 weeks after surgery. Bar = 5 mm.

Morphological findings visualised either by confocal microscopy (Fig. 3F) or by fluorescence microscopy show that the SYs and ACs were randomly distributed without any particular pattern, independent of the cell component ratio, in all structures. The morphologic appearance of a completed spheroid structure after 36 h culture is shown under fluorescence microscopy in Fig. 4A.

For histological analysis, spheroids with various mixing ratios subjected to 3 days HDSS were evaluated with toluidine blue and safranin O staining. The cross sections of the spheroid samples elucidate the internal location and distribution of the cells and ECM such as proteoglycans and glycosaminoglycans. In addition, the results of immunohistochemistry for collagen ECM in the spheroids provide an indication of the degree of similarity with normal cartilaginous tissue. In the histological results, there were no prominent differences in the staining patterns among any of the specimens with differing cell component ratios. A normal phenotype for cartilage was indicated by both safranin O-positive glycosaminoglycan-rich areas and metachromatic sites, evoked by toluidine blue. However, the histological results found no spheroids with a normal cartilage phenotype, regardless of the cellular component ratio. In the cross-sectional area of all of the spheroids, ECM was sparsely and irregularly stained with safranin O and toluidine blue, suggesting a small amount of glycosaminoglycans and proteoglycans (Fig. 4A) and, furthermore, was positive for type I and type II collagen (Fig. 4A). Interestingly, this phenomenon also occurred for spheroids made up solely of ACs or SYs (0:100 SY:AC and 100:0 SY:AC).

**Gene expression**

To investigate the expression of type I and type II collagen, similar samples of spheroids with the five different mixing ratios were prepared to elucidate the effect of time during HDSS. Real time PCR analysis (RT-PCR) showed that both type I and type II collagen was expressed in each spheroid, regardless of cellular component ratio (Fig. 4B). The time courses (initiation *vs.* day 3) for mRNA expression of type I and type II collagen in the HDSS constructs showed an irregular pattern.

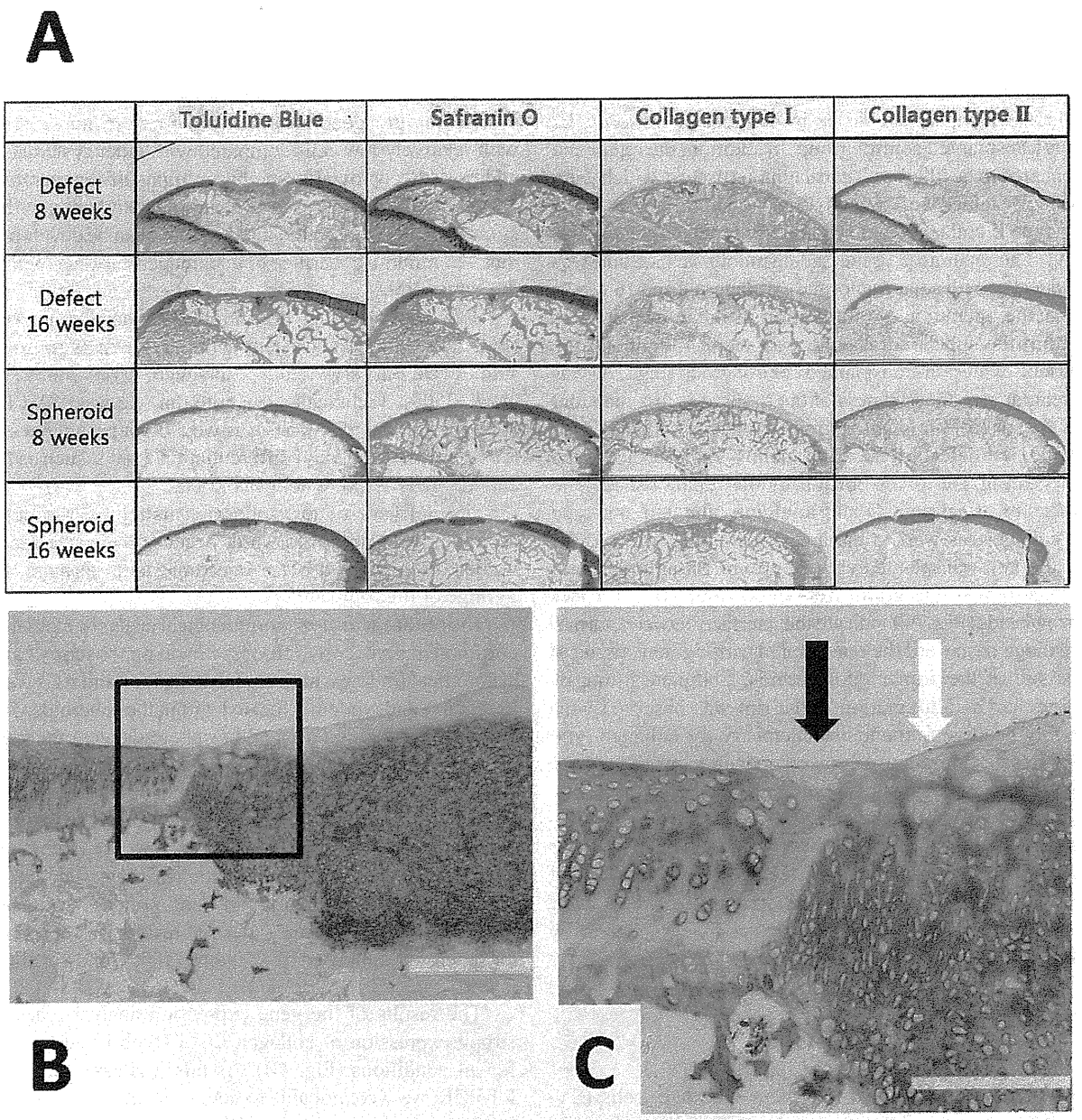


**Fig. 7.** Histological analyses. (**A**) Results for the *in vivo* study of toluidine blue and safranin O staining, and type I and type II collagen. Bar = 1 mm. (**B**) Histological observations of the implanted site 8 weeks after allotransplantation. Bar = 500 μm. (**C**) Magnified image of the black box. The black arrowhead indicates the interface between normal cartilage tissue and the regenerated tissue, and the white arrowhead indicates a chondrocyte clustering area. Bar = 200 μm.

**Examination of the transplanted spheroids**

As the optimal ratio of ACs and SYs for *in vivo* implantation, we selected 75:25 SY:AC spheroids for *in vivo* implantation study. We transplanted the 2- to 3-day spheroids to the total-thickness-defect model. It required 55.1 ±6.4 h to prepare the spheroidal transplants firm enough to be handled with micropipette aspiration, using HDSS for the implantation experiments. The operations were uneventful and all of the rabbits immediately resumed normal cage activity. No signs of arthritis, such as cartilage erosion or severe synovial proliferation, were observed in any of the knees that were operated on.

Based on macroscopic observations, the spheroid-implanted group had better integration of host cartilage, and the defects repaired by the spheroids were smoother than in the non-transplanted control group (Fig. 6). The defects in the spheroid-implanted group were filled with smooth white tissue compared with the non-transplanted control group. The borders of the reparative tissue were also visible and the colour of the tissue was slightly different from that of the surrounding normal cartilage. However, the defects in the non-transplanted control group remained empty or covered in reddish tissue. The global macroscopic scores for the spheroid-implanted group (6 knee joints) were

statistically better than (8 weeks; $p = 0.0130$, 16 weeks; $p = 0.0110$) those for the non-transplanted control group (6 knee joints) (Fig. 5A).

In the spheroid-implanted group, the defects were filled with reparative tissue in contrast to those of the non-transplanted control group. In addition, the repair site appeared to be filled with cartilaginous tissues, which were strongly stained with safranin O and toluidine blue, positive for type II collagen, and negative for type I collagen (Fig. 7A). The reparative tissue had a smooth surface and was connected with adjacent normal cartilage at 8 and 16 weeks after the operation. No infiltration of inflammatory cells within the subchondral bone was seen. In contrast, the surface of the non-transplanted control group (Fig. 7A) was irregular and the thickness of the tissue was less than that of the spheroid-implanted group. In the non-transplanted group, the defects were filled mainly with fibrous tissue concealing the lower portion of the repair tissue. The intensity of safranin O and toluidine blue and anti-type II collagen, as well as the areas of staining, were lower in the non-transplanted control group. Basal and lateral integration of the grafts were good (Fig. 7B, C). Black arrowheads (Fig. 7C) indicate the interface between normal cartilage tissue and the regenerated cartilaginous tissue at the site of the implanted spheroids. Complete filling of the defect and integration at the rim was observed with highly positive immunohistochemistry for collagen type II. A cluster formation of several chondrocytes around the interface of the regeneration area was observed (Fig. 7C). Furthermore, Wakitani's scores (Fig. 5B) for the spheroid-implanted group (6 knee joints) were significantly better than (8 weeks; $p = 0.0005$, 16 weeks; $p = 0.0278$) those of the control group (6 knee joints) at 8 and 16 weeks. The untreated defects had poorer scores at 8 weeks than at 16 weeks.

## Discussion

Since synovium-derived mesenchymal stem cells (SY-MSCs) were first identified and successfully isolated in 2001 (De Bari *et al.*, 2001) as a new origin among MSC families, they have been increasingly regarded as a versatile therapeutic cell species for musculoskeletal regeneration, particularly for reconstruction of cartilage, bone, adipose tissue, tendons, muscles, etc. In addition to having general multipotency in common with the MSC community, SY-MSCs excel compared to other-sourced MSCs in their higher proliferation and superiority in chondrogenesis (Sakaguchi *et al.*, 2005; Fan *et al.*, 2009). Furthermore, their multipotent capacity is not influenced by donor age, cell passages, or cryopreservation (De Bari *et al.*, 2001).

In this study, we chose SYs as a partial replacement for ACs as a mixture component, and were able to fabricate mixed SY-AC constructs as spheroid aggregates. SYs appear to be a promising cell source for cartilage regeneration, since synovium-derived cells have also been chosen as a substantial source for chondrogenesis (Shimomura *et al.*, 2010). Compared to other sources of MSCs, SY-MSCs show higher proliferative and chondrogenic ability, and large amounts of SY-MSCs can be easily obtained from small amounts of synovial tissue. In clinical applications, cell numbers obtained from biopsies are quite limited, and there are disadvantages in performing cell proliferation with AC alone. The HDSS system rapidly generates scaffold-free artificial tissue with relatively few cells compared with other systems. In addition, the synovial tissue has a high self-regenerative ability. When SYs are used as a partial cell component for clinical ACI, it is expected that a method can be developed that will minimise sacrifice of undamaged cartilage within the same joint.

SYs display higher proliferative capacity than ACs (Fig. 2B), which is consistent with the results of previous studies (De Bari *et al.*, 2001; Sakaguchi *et al.*, 2005; Fan *et al.*, 2009). Technically, we note that we used SYs for HDSS rather than SY-MSCs, as we did not prove that our SYs were SY-MSCs and differentiation assays, such as for chondrogenesis, were not performed.

The delivery of the spheroids using micropipette aspiration was straightforward, because their size range was small enough to place injectable units through the syringe or micropipette tips.

The results of *in vitro* morphological analysis, including confocal microscopy, fluorescence microscopy, and histological findings, indicated that the SYs and ACs were irregularly and randomly located within the spheroids. The phenotypes of the interior of the spheroids were far from the normal cartilage phenotype regardless of the cellular component ratio. The ECM was defective and sparsely stained with safranin O and toluidine blue in addition to insufficient intensity of positive staining for type I and type II collagen in immunohistochemistry, suggesting small amounts of glycosaminoglycans, proteoglycans, and collagen fibres. The same pattern of results was observed for spheroids composed of AC alone (100:0) and SY alone (0:100).

The results of the gene expression analysis showed strong expression of collagen ECM (type I and type II) for all conditions (Fig. 4B). As this was assessed using RT-PCR, we were not able to determine the exact relative levels of expression of the ECM gene for all conditions. Additional analyses, such as RT-PCR, are needed to quantify exactly the relative expression level of ECM among the different cellular ratios. We suppose that there are several explanations for the different results of ECM expression obtained using histological analysis and RT-PCR. Although we can speculate that the real accumulation of ECM secreted by the cells in each spheroid does not always correspond to the results of the RT-PCR analysis, these are mere ECM mRNA expression levels, which do not always coincide with the real secretion of the ECM protein after translation. Therefore, the difference between the immunohistochemistry and RT-PCR results regarding ECM levels may represent differences between the levels of transcription and translation of ECM. We are not certain of the reason for this discordance at present. Shear stress resulting from HDSS may be related to this phenomenon. However, we need to perform additional analyses to verify the reasons for this discrepancy substantially. Conversely, as histological analysis only provides fragmentary information of spheroids, 2D cross sections of spheroids

have, thus far, been limited for 3D spheroids that exhibit random distribution of ACs and SYs. In addition, the results of the RT-PCR analysis reflect the complete information of 3D spheroids.

Chondrocyte 3D culture techniques such as pellet culture, bioreactor culture have been developed to obtain a large amount of cultured cells with a well-maintained cartilage phenotype. Manipulation of the culturing environment for chondrocytes presents the most feasible mechanism for optimising cell behaviour and phenotype (Lin *et al.*, 2006). Using an ordinary pellet culture, after 2 weeks, the ECM in the pellets was comparable with that of normal cartilage. Chondrocyte redifferentiation from monolayer-cultured chondrocytes has been demonstrated to occur in neocartilage over 14 days (Zhang *et al.*, 2004). However, our scaffold-free spheroids are still immature *de novo* cartilage grafts, which are expected to regenerate into normal cartilaginous tissue *in situ* and *in vivo* within full-thickness osteochondral defects as soon as they are prepared through HDSS. The HDSS period (2-3 days) in the present study was shorter than usual *in vitro* culture length for chondrogenesis (14-21 days). It is suggested that neo-cartilage in 3D culture is observed after 14-21 days of continuous culture. Together with the previous literature, this reflected the fact that the duration of our 3D culture was too short to allow re-differentiation from the monolayer culture of ACs and SYs passaged continuously (Nagase *et al.*, 2008; Zhang *et al.*, 2004). Furthermore, our system can yield mass production of transplantable chondrogenic tissue. However, most of the pellet culture systems are not designed to produce transplantable tissue; rather, they are an analytical tool that usually leads to the formation of a single aggregate per experiment.

The co-culture of ACs and MSCs has gained considerable attention recently. Monolayer co-culture of immortalised human ACs with immortalised human MSCs in the absence of exogenous TGF-β resulted in chondrocytic differentiation of the MSCs, based on collagen type II protein expression (Chen *et al.*, 2009), and the MSCs were committed to chondrocytes, which are influenced by the cellular microenvironment and the paracrine signals of chondrocytes (Grassel and Ahmed, 2007). The HDSS system provides this radical microenvironment to MSCs from ACs. However, we suggest that our HDSS culture system shortens the preparation time for fabricating a considerable quantity of spheroids, and can substantially shorten the total time required for an *ex vivo* procedure. Moreover, a high-density culture of chondrocytes, which promotes cell to-cell contact, has been significantly associated with extracellular matrix biosynthesis (Watt, 1988). In the present study, ACs and SYs were cultured together in a high-density suspension state on a non-adhesive culture plate while maintaining continuous suspension conditions; the cells then adhered to each other to develop spheroidal cell mixtures, producing limited ECM due to the short culture time. The molecular mechanism for cell adhesion under rapid formation of spheroid may involve several molecules such as integrins (α10, α3, and β1) (Gigout *et al.*, 2009; Mitani *et al.*, 2009; Shimaya *et al.*, 2010), fibronectin (Mitani *et al.*, 2009), N-cadherins (Djouad *et al.*, 2007; Quintana *et al.*, 2009).

However, in general, a high-density culture may limit the amount of mass transfer. At present, our system, with a product size small enough for injection, is superior for delivering transplants. In the animal experiments, articular cartilage defects in which SY-AC spheroids were implanted *in vivo* showed improved histological findings (Figs. 5B and 7). The allografted spheroidal aggregates differentiated slowly to chondrocytes in the articular cartilage defects and produced an extracellular matrix similar to that of hyaline cartilage, thereby maintaining the chondrocyte phenotype. The implanted spheroids exhibited proliferation and differentiation activity in the articular cartilage defects, resulting in the formation of hyaline cartilage.

No signs were observed of immunologic rejection or degeneration of the reparative tissue during the observation period. As a potential limitation of the present study, we did not perform detailed laboratory investigations to detect specific immunologic reactions such as development of antibodies or cell-mediated responses.

We choose 75:25 SY:AC spheroids to transplant for cartilage regeneration. According to the previous literature (Ochi *et al.*, 2002; Shimomura *et al.*, 2010), spheroids composed of AC alone and SY alone may have the potential to produce hyaline cartilage for *in vivo* implantation, furthermore, other ratios of SY:AC may also have the potential to produce reparative tissue for regenerate cartilage; however, In the view point of utility of SYs as a partial replacement for ACs in ACI, we applied this ratio (75:25) in the present implantation study since this formation maximise the merit and efficacy of using SYs of high proliferation with less invasive procedure and donor site morbidity among other SY:AC ratios. Further *in vivo* studies is needed to determine the exact nature of implanted spheroids including transplantation with different other ratios of SY:AC and monitoring the transplants fate with fluorescent labelling.

Interestingly, numerous cluster formations of chondrocytes near the interface with the regenerative tissue were observed. This clustering phenomenon is a sign of repair in early osteoarthritis (Frenkel and Di Cesare, 1999). This result indicates that scaffold-free spheroids inserted into osteochondral defects show high regenerative capacity. Koga *et al.* (2008b) described the viscosity and adhesive properties of SYs in an *ex vivo* analysis in rabbits and demonstrated that the number of attached cells increased in a time-dependent manner; more than 60 % of the cells attached within 10 min under normal gravity. Similarly, we held the defects stationary after implantation for more than 10 min (15 min) without additional fixation such as a periosteal patch. Accordingly, dislocation of spheroids and leakage from the implanted sites were minimal. The present results are consistent to some extent with the earlier report (Koga *et al.*, 2008b). However, the mechanical strength properties of regenerated articular cartilage still remain to be investigated through *in vivo* studies on larger animals (i.e., sheep or pigs).

We confirmed that in the early stage of transplantation, effective restoration of articular cartilage is seen with reparative mixed cells derived from MSCs and ACs, which can induce recruited MSCs into ACs and trigger chondrogenesis (Kaneshiro *et al.*, 2006; Nagai *et al.*,

2008b), and achieved good restoration results over the long term. We therefore hypothesised that good cartilage repair may be achieved by providing a proper quantity of an initiator (ACs) and a comparable quantity of materials (SY-MSCs or bone marrow-derived MSCs) to induced ACs in the osteochondral defect, no matter whether it is full-thickness or partial.

To the best of our knowledge, no previous studies have demonstrated the feasibility of cellular transplants consisting of different cells or origins of cells. The HDSS maintains ACs and SYs in a high-density suspension for a short period of time and yields 3D minimal building units of spheroids. Frequent cell-cell contact, as permitted by growth at high density, stimulates the formation of aggregates. This technology may have an advantage in a clinical setting, because it is scaffold-free and uses no artificial substances. With this new technique, broad lesions can be treated free of scaffolds and artificial biomaterials. Effective use of SYs and minimal invasiveness are anticipated advantages of this novel method for replacement of chondrocytes in ACI.

## Conclusions

Using the HDSS method, we can successfully prepare a large quantity of cellular spheroids in a short period using mixed ACs and SYs, whose high proliferation potency and differentiation potency does not change. The allografted grafts exhibited differential activity to chondrocytes showing *in vivo* extracellular matrix production. These results suggest an ability to achieve regeneration of articular cartilage through implantable spheroids as a therapeutic minimal building unit.

## Acknowledgements

The authors thank Dr. Ichiro Sekiya (Section of Cartilage Regeneration, Graduate School, Tokyo Medical and Dental University, Japan) for providing useful information, comments, and technical critique with respect to primary culturing of synovium-derived cells, whose MSC characteristics had previously been reported by his group (Koga *et al.*, 2007; Koga *et al.*, 2008a).

This research was supported by Grant-in-Aid for Challenging Exploratory Research from Ministry of Education, Culture, Sports, Science and Technology in Japan and Basic Science Research Program through the National Research Foundation of Korea (NRF) funded by the Ministry of Education, Science and Technology (2010-0024188).

## References

Anderson JM, Rodriguez A, Chang DT (2008) Foreign body reaction to biomaterials. Semin Immunol **20**: 86-100.

Badylak SF, Gilbert TW (2008) Immune response to biologic scaffold materials. Semin Immunol **20**: 109-116.

Brehm W, Aklin B, Yamashita T, Rieser F, Trub T, Jakob RP, Mainil-Varlet P (2006) Repair of superficial osteochondral defects with an autologous scaffold-free cartilage construct in a caprine model: implantation method and short-term results. Osteoarthritis Cartilage **14**: 1214-1226.

Brittberg M, Lindahl A, Nilsson A, Ohlsson C, Isaksson O, Peterson L (1994) Treatment of deep cartilage defects in the knee with autologous chondrocyte transplantation. N Engl J Med **331**: 889-895.

Buckwalter JA, Mankin HJ (1998) Articular cartilage: Degeneration and osteoarthritis, repair, regeneration, and transplantation. Instr Course Lect **47**: 487-504.

Chen WH, Lai MT, Wu AT, Wu CC, Gelovani JG, Lin CT, Hung SC, Chiu WT, Deng WP (2009) *In vitro* stage-specific chondrogenesis of mesenchymal stem cells committed to chondrocytes. Arthritis Rheum **60**: 450-459.

Cook SD, Patron LP, Salkeld SL, Rueger DC (2003) Repair of articular cartilage defects with osteogenic protein-1 (BMP-7) in dogs. J Bone Joint Surg Am **85-A Suppl 3**: 116-123.

Darling EM, Athanasiou KA (2003) Articular cartilage bioreactors and bioprocesses. Tissue Eng **9**: 9-26.

De Bari C, Dell'Accio F, Tylzanowski P, Luyten FP (2001) Multipotent mesenchymal stem cells from adult human synovial membrane. Arthritis Rheum **44**: 1928-1942.

Djouad F, Delorme B, Maurice M, Bony C, Apparailly F, Louis-Plence P, Canovas F, Charbord P, Noel D, Jorgensen C (2007) Microenvironmental changes during differentiation of mesenchymal stem cells towards chondrocytes. Arthritis Res Ther **9**: R33.

Fan J, Varshney RR, Ren L, Cai D, Wang DA (2009) Synovium-derived mesenchymal stem cells: a new cell source for musculoskeletal regeneration. Tissue Eng Part B Rev **15**: 75-86.

Freed LE, Grande DA, Lingbin Z, Emmanual J, Marquis JC, Langer R (1994) Joint resurfacing using allograft chondrocytes and synthetic biodegradable polymer scaffolds. J Biomed Mater Res **28**: 891-899.

Frenkel SR, Di Cesare PE (1999) Degradation and repair of articular cartilage. Front Biosci **4**: D671-685.

Furukawa KS, Suenaga H, Toita K, Numata A, Tanaka J, Ushida T, Sakai Y, Tateishi T (2003) Rapid and large-scale formation of chondrocyte aggregates by rotational culture. Cell Transplant **12**: 475-479.

Gigout A, Buschmann MD, Jolicoeur M (2009) Chondrocytes cultured in stirred suspension with serum-free medium containing pluronic-68 aggregate and proliferate while maintaining their differentiated phenotype. Tissue Eng Part A **15**: 2237-2248.

Grassel S, Ahmed N (2007) Influence of cellular microenvironment and paracrine signals on chondrogenic differentiation. Front Biosci **12**: 4946-4956.

Iwasa J, Engebretsen L, Shima Y, Ochi M (2009) Clinical application of scaffolds for cartilage tissue engineering. Knee Surg Sports Traumatol Arthrosc **17**:561-577.

Kaneshiro N, Sato M, Ishihara M, Mitani G, Sakai H, Mochida J (2006) Bioengineered chondrocyte sheets may be potentially useful for the treatment of partial thickness defects of articular cartilage. Biochemical and biophysical research communications **349**: 723-731.

Koga H, Muneta T, Ju YJ, Nagase T, Nimura A, Mochizuki T, Ichinose S, von der Mark K, Sekiya I (2007) Synovial stem cells are regionally specified according to local microenvironments after implantation for cartilage regeneration. Stem Cells **25**: 689-696.

Koga H, Muneta T, Nagase T, Nimura A, Ju YJ, Mochizuki T, Sekiya I (2008a) Comparison of mesenchymal tissues-derived stem cells for *in vivo* chondrogenesis: suitable conditions for cell therapy of cartilage defects in rabbit. Cell and tissue research **333**: 207-215.

Koga H, Shimaya M, Muneta T, Nimura A, Morito T, Hayashi M, Suzuki S, Ju YJ, Mochizuki T, Sekiya I (2008b) Local adherent technique for transplanting mesenchymal stem cells as a potential treatment of cartilage defect. Arthritis Res Ther **10**: R84.

Lee JI (2007) Transplants encapsulated with eelf-elastic cartilage and method of preparing the same. WO 2008/002059. World Intellectual Property Organization International Bureau, International application published under the Patent Cooperation Treaty (PCT).

Lin Z, Willers C, Xu J, Zheng MH (2006) The chondrocyte: biology and clinical application. Tissue Eng **12**: 1971-1984.

Masuoka K, Asazuma T, Ishihara M, Sato M, Hattori H, Yoshihara Y, Matsui T, Takase B, Kikuchi M, Nemoto K (2005) Tissue engineering of articular cartilage using an allograft of cultured chondrocytes in a membrane-sealed atelocollagen honeycomb-shaped scaffold (ACHMS scaffold). J Biomed Mater Res B Appl Biomater **75**: 177-184.

Mitani G, Sato M, Lee JI, Kaneshiro N, Ishihara M, Ota N, Kokubo M, Sakai H, Kikuchi T, Mochida J (2009) The properties of bioengineered chondrocyte sheets for cartilage regeneration. BMC Biotechnol **9**: 17.

Mochizuki T, Muneta T, Sakaguchi Y, Nimura A, Yokoyama A, Koga H, Sekiya I (2006) Higher chondrogenic potential of fibrous synovium- and adipose synovium-derived cells compared with subcutaneous fat-derived cells: distinguishing properties of mesenchymal stem cells in humans. Arthritis Rheum **54**: 843-853.

Nagai T, Furukawa KS, Sato M, Ushida T, Mochida J (2008a) Characteristics of a scaffold-free articular chondrocyte plate grown in rotational culture. Tissue Eng Part A**14**: 1183-1193

Nagai T, Sato M, Furukawa KS, Kutsuna T, Ohta N, Ushida T, Mochida J (2008b) Optimization of allograft implantation using scaffold-free chondrocyte plates. Tissue Eng Part A **14**: 1225-1235.

Nagase T, Muneta T, Ju YJ, Hara K, Morito T, Koga H, Nimura A, Mochizuki T, Sekiya I (2008) Analysis of the chondrogenic potential of human synovial stem cells according to harvest site and culture parameters in knees with medial compartment osteoarthritis. Arthritis Rheum **58**: 1389-1398.

Nehrer S, Domayer S, Dorotka R, Schatz K, Bindreiter U, Kotz R (2006) Three-year clinical outcome after chondrocyte transplantation using a hyaluronan matrix for cartilage repair. Eur J Radiol **57**: 3-8.

Nimura A, Muneta T, Koga H, Mochizuki T, Suzuki K, Makino H, Umezawa A, Sekiya I (2008) Increased proliferation of human synovial mesenchymal stem cells with autologous human serum: comparisons with bone marrow mesenchymal stem cells and with fetal bovine serum. Arthritis Rheum **58**: 501-510.

Ochi M, Uchio Y, Kawasaki K, Wakitani S, Iwasa J (2002) Transplantation of cartilage-like tissue made by tissue engineering in the treatment of cartilage defects of the knee. J Bone Joint Surg Br **84**: 571-578.

Ochi M, Uchio Y, Tobita M, Kuriwaka M (2001) Current concepts in tissue engineering technique for repair of cartilage defect. Artif Organs **25**: 172-179.

Pittenger MF, Mackay AM, Beck SC, Jaiswal RK, Douglas R, Mosca JD, Moorman MA, Simonetti DW, Craig S, Marshak DR (1999) Multilineage potential of adult human mesenchymal stem cells. Science **284**: 143-147.

Prockop DJ (1997) Marrow stromal cells as stem cells for nonhematopoietic tissues. Science **276**: 71-74.

Quintana L, zur Nieden NI, Semino CE (2009) Morphogenetic and regulatory mechanisms during developmental chondrogenesis: new paradigms for cartilage tissue engineering. Tissue Eng Part B Rev **15**: 29-41.

Sakaguchi Y, Sekiya I, Yagishita K, Muneta T (2005) Comparison of human stem cells derived from various mesenchymal tissues: superiority of synovium as a cell source. Arthritis Rheum **52**: 2521-2529.

Samlowski WE, Robertson BA, Draper BK, Prystas E, McGregor JR (1991) Effects of supravital fluorochromes used to analyze the in vivo homing of murine lymphocytes on cellular function. J Immunol Methods **144**: 101-115.

Sekiya I, Larson BL, Smith JR, Pochampally R, Cui JG, Prockop DJ (2002) Expansion of human adult stem cells from bone marrow stroma: conditions that maximize the yields of early progenitors and evaluate their quality. Stem Cells **20**: 530-541.

Shimaya M, Muneta T, Ichinose S, Tsuji K, Sekiya I (2010) Magnesium enhances adherence and cartilage formation of synovial mesenchymal stem cells through integrins. Osteoarthritis and cartilage / OARS, Osteoarthritis Res Soc **18**: 1300-1309.

Shimomura K, Ando W, Tateishi K, Nansai R, Fujie H, Hart DA, Kohda H, Kita K, Kanamoto T, Mae T, Nakata K, Shino K, Yoshikawa H, Nakamura N (2010) The influence of skeletal maturity on allogenic synovial mesenchymal stem cell-based repair of cartilage in a large animal model. Biomaterials **31**: 8004-8011.

Wakitani S, Imoto K, Yamamoto T, Saito M, Murata N, Yoneda M (2002) Human autologous culture expanded bone marrow mesenchymal cell transplantation for repair of cartilage defects in osteoarthritic knees. Osteoarthritis Cartilage **10**: 199-206.

Watt FM (1988) Effect of seeding density on stability of the differentiated phenotype of pig articular chondrocytes in culture. J Cell Sci **89**: 373-378.

Yoshimura H, Muneta T, Nimura A, Yokoyama A, Koga H, Sekiya I (2007) Comparison of rat mesenchymal stem cells derived from bone marrow, synovium, periosteum, adipose tissue, and muscle. Cell Tissue Res **327**: 449-462.

Zhang Z, McCaffery JM, Spencer RG, Francomano CA (2004) Hyaline cartilage engineered by chondrocytes

in pellet culture: histological, immunohistochemical and ultrastructural analysis in comparison with cartilage explants. J Anat **205**: 229-237.

**Discussion with Reviewers**

**Reviewer I**: The results showed that there was no noticeable difference in the chondrogenic matrix synthesis in any AC/SY combination and that the matrix formed was not particularly chondrogenic. Please comment.
**Authors**: As there was no noticeable difference in the synthesis of the chondrogenic matrix in any AC/SY combination in the present study, we chose an SY:AC ratio of 75:25 for spheroids based on the utility of SYs as a partial replacement for ACs. This formation maximised the merit and efficacy of using SYs of high proliferation with less invasive procedure and donor site morbidity among other cellular ratios using SYs based on quantity of tissue demanded. In this study, the matrix formed did not seem particularly chondrogenic in the *in vitro* condition; however, our scaffold-free spheroids were confirmed as being an immature state of cartilage grafts, which are expected to regenerate into normal cartilaginous tissue *in situ* and *in vivo*.

**Reviewer I**: Has any type of X immunofluorescence been carried out?
**Authors**: In this study, we have not performed immunohistochemistry for type X collagen in the spheroids that are associated with chondrocyte hypertrophy and matrix mineralisation. However, we think that this immunohistochemistry is worth performing to obtain precise information on the state of spheroids regardless of the duration of the *in vitro* culturing of cartilaginous tissue.

**Reviewer I**: Does the PKH26 remain evident in the processed samples? If so, could you use this to detect which cells have contributed to repair or could another marker be used that will allow the cells to be tracked during defect repair? This would also show if cells have migrated from the bone marrow as the defect penetrated the sub-chondral bone.
**Authors**: Yes, obviously the PKH fluorescent cell linker dye remained in the processed samples for in vitro evaluation of the morphology and distribution of cells within the spheroids of mixed ACs and SYs. However, we have not performed *in vivo* tracing using this fluorescent dye, as mentioned previously. In addition, similarly, we could use a specific marker that allows the tracking of cells that migrated from the bone marrow during the repair of the defect. However, we have not performed this experiment either. Further experiments regarding this curiosity will be expected to reveal the exact mechanism involving ACs, SYs and cells from bone marrow that represents the complicated phenomenon of cartilage regeneration.

**Reviewer I**: If the spheroids were kept in culture for a longer time period, are any differences seen in matrix production between the different ratios of AC/SY cells?
**Authors**: In this study, we did not perform long-term culture (over 3 days) with the spheroids kept in the HDSS culture system. However, we expect chondrogenesis of spheroids in the 3D HDSS culture condition with an extended culturing period (over 2-3 weeks) (Zhang *et al.*, 2004, text reference). Our culture system yields a similar state of 3D culture, such as pellet culture, but this system gives rise additionally to shearing stress generated by the circular flow of the culture medium. Therefore, we expect that our system differs from ordinary 3D cultures. Additional comparative studies between our method and conventional 3D culture methods are needed to establish the differences, and such studies are being carried out at present.

# The Influence of Ho:YAG Laser Irradiation on Intervertebral Disc Cells

**Masato Sato, MD, PhD,[1]* Miya Ishihara, PhD,[2] Makoto Kikuchi, PhD,[2] and Joji Mochida, MD, PhD[1]**

[1]*Department of Orthopaedic Surgery, Surgical Science, Tokai University School of Medicine, 143 Shimokasuya, Isehara, 259-1193 Kanagawa, Japan*

[2]*Department of Medical Engineering, National Defense Medical College, 3-2 Namiki, Tokorozawa, 359-8513 Saitama, Japan*

**Background and Objective:** Various types of laser have been reported for percutaneous laser disc decompression (PLDD). The aim of this study was to understand the effects on intervertebral disc cells following Ho:YAG laser irradiation, using a three-dimensional culture model, and consider appropriate irradiation conditions.

**Study Design/Materials and Methods:** Intervertebral discs from the lumbar spine were obtained from 36 female Japanese white rabbits and processed to obtain isolated cells in three-dimensional cultures. Photoacoustic and photothermal effects were investigated by irradiating three-dimensional cultures with Ho:YAG laser at 27 or 54 J. Residual cell counts after irradiation were estimated based on DNA content according to fluorometric assay. Lactate dehydrogenase levels were also investigated as a marker of damage to cell plasma membranes. Finally, proteoglycan synthesis was measured by rapid filtration assay of $^{35}S$ incorporation, as an index of matrix synthesis.

**Results:** Residual cell count tended to be higher in the 27-J group. Plasma membrane damage was higher and remained high longer after irradiation in the 54-J group. Proteoglycan synthesis was higher in the 27-J group than in the 54-J group, with some conditions (e.g., 90 mJ/pulse condition) showing marked activation of proteoglycan synthesis maintained for a long time after irradiation.

**Conclusions:** Three-dimensional culture models of intervertebral disc cells are useful for clarifying relationships between cell reactions and photoacoustic and photothermal effects after laser irradiation. Total energy is closely related to optimization of irradiation conditions, which may allow optimization of cytoprotection and promotion of matrix synthesis in clinical practice. Lasers Surg. Med. 43:921–926, 2011. © 2011 Wiley Periodicals, Inc.

**Key words:** percutaneous laser disc decompression; three dimensional culture; intervertebral disc cell; irradiation condition

## INTRODUCTION

Percutaneous laser disc decompression (PLDD) is effective in cases of subligamentous extrusion-type intervertebral disc herniation in which high pressure is maintained within the disc. Various types of laser for PLDD have been reported at the clinical or experimental level, including Nd:YAG laser [1–3], frequency doubled Nd:YAG laser (KTP:YAG) [4], Ho:YAG laser [5,6], and semiconductor laser [7]. This indicates the high interest in lasers as a low-invasive treatment for intervertebral disc hernia.

We report a series of studies to identify appropriate irradiation conditions using Ho:YAG laser. Compared with Nd:YAG laser, which has the characteristics of a coagulation laser, Ho:YAG offers superior tissue vaporization and a much lower thermal effect. Even with Ho:YAG laser, however, the effect on cells is substantial, and the appropriate irradiation conditions we describe here are conditions under which the adverse effects from photothermal and photoacoustic influences are small and the self-repair ability of tissue is activated.

Nd:YAG laser is the most commonly used type of laser in PLDD. With a wavelength of 1.064 μm, this laser can reach deep into tissue, up to several centimeters depending on power. This means that careful thought must be given to coagulation and necrosis beyond the range of irradiation. In contrast, Ho:YAG laser has a wavelength of 2.1 μm and reaches a depth in tissue of $\leq$ 0.5 mm [8–10]. Tissue permeability is low, tissue vaporization is excellent, and the effect on surrounding tissue is minimal. With Nd:YAG laser, the tissue vaporization that occurs with Ho:YAG laser is not seen, and with laser irradiation of small enclosed spaces like that within intervertebral discs, greater tissue damage tends to result from heat retention. From an investigation of 387 patients before and after laser disc decompression, Tonami et al. [11] reported osteonecrosis in an adjacent vertebra in four patients based on magnetic resonance imaging. Adverse effects on the intervertebral disc and vertebral body also occurred with this method, causing strong low back pain that had not been present preoperatively. Another report described a patient who experienced intense pain in a

*Corresponding to: Masato Sato, MD, PhD, Department of Orthopaedic Surgery, Surgical Science, Tokai University School of Medicine, 143 Shimokasuya, Isehara, Kanagawa 259-1193, Japan. E-mail: sato-m@is.icc.u-tokai.ac.jp

Accepted 10 August 2011
Published online 15 October 2011 in Wiley Online Library (wileyonlinelibrary.com).
DOI 10.1002/lsm.21120

lower limb during laser disc decompression, and who displayed considerable enlargement and burn scar of the nerve root of that disc in an additional microscopic discectomy conducted 4 weeks later [12]. The need for salvage operation after PLDD has also been reported [13]. Investigation of appropriate laser irradiation conditions is thus very important from the perspective of preventing adverse effects. We have studied the effects of laser irradiation on intervertebral disc cells using a three-dimensional culture model of intervertebral disc cells [14,15].

If the indications are strictly selected and the procedure is performed properly, PLDD offers a low-invasive surgical method for intervertebral disc hernia. However, despite extensive reading we have seen no studies on irradiation conditions that have focused on post-irradiation cell reactions. The aim of this study was to understand the effects on intervertebral disc cells following Ho:YAG laser irradiation, using a three-dimensional culture model, and consider appropriate irradiation conditions.

## MATERIALS AND METHODS

### Preparation of Three-Dimensional Culture

Intervertebral discs from the lumbar spine were obtained from 36 female Japanese white rabbits weighing about 1 kg. Intervertebral discs were shredded with scissors and digested in Dulbecco's modified Eagle's medium (DMEM) (Nissui Pharmaceutical, Tokyo, Japan) containing 0.2% (w/v) pronase E (Kaken, Tokyo, Japan) for 1 hour and then in DMEM containing 0.025% (w/v) bacterial collagenase P (Boehringer Mannheim, Mannheim, Germany) for 4 hours (16). The digested tissue was passed through a cell strainer (Becton Dickinson Labware, Franklin Lakes, NJ) with a pore size of 40 μm. The filtrate was centrifuged at 1,500 rpm for 5 minutes. Isolated cells were washed three times with DMEM. The cells were seeded in 96-well culture plates at cell densities of $1 \times 10^6$/ml and incubated within 1% agarose gel containing DMEM supplemented with 10% fetal bovine serum (Gibco BRL, Grand Island, NY). An equal amount of the medium was added onto the gel at 37°C in an atmosphere of 5% $CO_2$ and 95% air.

### Experimental Setup for Monitoring of Photoacoustic and Photothermal Effect

The Ho:YAG laser used (SEO1-2-3 HO2100; Schwartz Electro-Optics,. Inc., Orlando, FL) had a wavelength of 2.1 μm and pulse width of 250 μseconds. Cells were divided by the total energy (= laser energy × pulse number of shots) used into a 27-J group and 54-J group for the investigation. Parameters were fiber tip irradiation energy of 40–180 mJ/pulse, shot number varied from 150 to 1,350, repetition rate of 5 Hz, and total energy at the given levels.

The setup consisted of Ho:YAG laser guided to a quartz glass fiber (diameter, 200 μm), and irradiation from the surface of a three-dimensional culture model with the medium removed (Fig. 1). The irradiation condition in clinical settings is set as "the amount of energy that can vaporize 1 g of nucleus pulposus" and total energy was scaled out from there for application to the experimental system. The experiment was conducted at 54 J, which is close to clinical conditions, and at half that amount, 27 J. Irradiation conditions were photoacoustics measured via piezoelectric film PVdF film (Durapore PVDF 5UM WH PL47MM 100/PK; Millipore, Billerica, MA) and photothermal effect monitored using thermography (Neo Thermo TVS-620; NipponAvionics Co., Ltd., Tokyo, Japan). Agarose gel containing chondrocytes that had been incubated on a 96-well plate (diameter: 6.4 mm × height: 10 mm) was removed from the plate and placed so that the fiber ends and the center part of the agarose

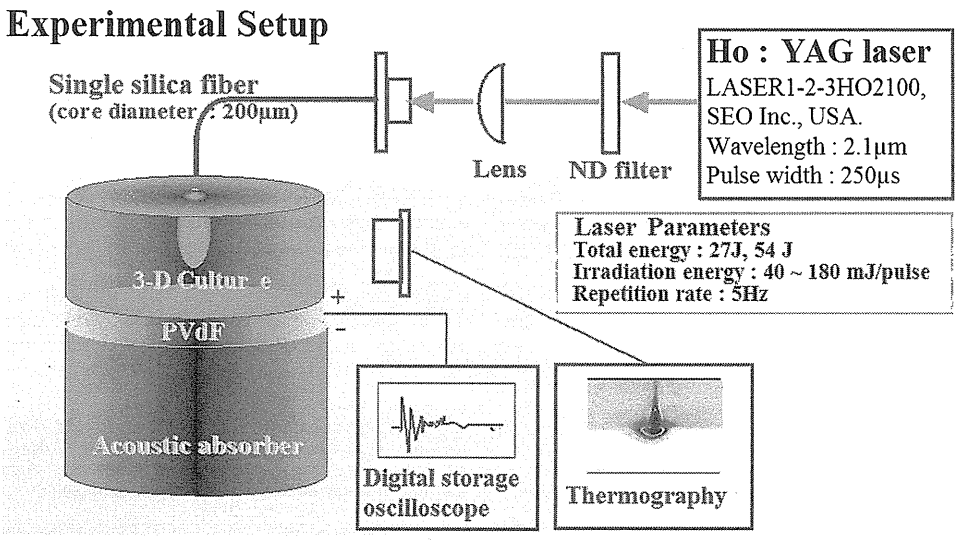


Fig. 1. Experimental setup.

gel surface were barely touching. The state under laser irradiation was measured from the true lateral surface of the gel by direct thermography at the distance of 30 cm from the lateral surface of the gel. Thus, we accomplished 2-D temperature mapping of the gel. Tests were performed with a sample size of $n = 8$ in each group at three different stress amplitudes and thermal loads.

As the effect from photoacoustics, stress amplitude ($P(t)$) was calculated from Equations (1) and (2) below with piezoelectric film data [16]:

$$F(t) = \frac{V(t) \times (Cd + Cp)}{dt} \quad (1)$$

$$P(t) = 54.2 \times V(t) \quad (2)$$

$F(t)$, detected stress at transducer; $V(t)$, output voltage of transducer; $Cd$, loading capacitance of oscilloscope; $Cp$, capacitance of transducer; $dt$, strain constant for PVdF.

For photoacoustics, thermal load ($\Omega$) was defined as in Equation (3) below and calculated by integrating the volume of the portion that reached a temperature $\geq$50°C on thermography [15]:

$$\Omega = \int (> =''°\text{C volume ratio})\delta\tau \quad (3)$$

### DNA Content as a Marker of Residual Cells

DNA content was used as an index of residual cell count in wells. Cells were harvested after irradiations and treated with a papain solution at 60°C overnight. The papain solution was prepared by dissolving papain at a concentration of 125 μg/ml in 0.1 M phosphate-buffered saline (pH 6.0) with 5 mM cysteine–HCI and 5 mM $Na_2$ EDTA. The DNA content in specimens was then determined according to the methods of Kim et al. [17] by fluorometric assay using Hoechst 33258 (Polyscience, Warrington, PA).

### Evaluation of Damage to the Plasma Membrane

Lactate dehydrogenase (LDH) is a stable cytoplasmic enzyme present in all cells, and is rapidly released into the cell culture supernatant upon damage to the plasma membrane. Levels of this enzyme thus reflect loss of membrane integrity and offer an indicator of cell death. Using a Cytotoxicity Detection Kit (Boehringer Mannheim), LDH release was measured in culture supernatants by enzyme-linked immunosorbent assay [18,19]. This test was performed with a sample size of $n = 8$ in each group. LDH rate was calculated according to formula (4):

$$\text{LDH realease (\%)} = \frac{[\text{experimental value} - \text{low control value}]}{[\text{high control value} - \text{low control value}]} \times 100 \quad (4)$$

### Evaluation of Matrix Synthesis Ability

Proteoglycan synthesis was used as an index of matrix synthesis, and was measured by rapid filtration assay of $^{35}S$ incorporation [20]. The three-dimensionally cultured cells and DMEM containing $^{35}S$-sulfate at 10 μCi/ml were incubated for every 12 hours (12-hour pulse labeling) from 0 to 48 hours after laser irradiation, and quantified by scintillation counting. This assay was applied to measure the matrix-synthesizing ability of damaged target cells. This test was performed with a sample size of $n = 8$ in each group.

## RESULTS

### Residual Cell Count

When the amount of vaporization from the laser is large, the residual cell count (%DNA content) is low. In the 54-J total energy group, this value was 60–70%, and tended to decrease as the amount of energy per shot increased. In the 27-J group, in contrast, %DNA content was about 80% in all cases. Residual cell count thus tended to be higher in the 27-J group with a small amount of vaporization (Fig. 2).

### Cell Damage

In the 27-J group, LDH release was 10–35% and the injury to cells was mild. The value was particularly low 12 hours after irradiation, at about 10% in all cases, and little cytotoxicity was evident. In the 54-J group, high values of $\geq$40% were seen from 12 hours after irradiation, reaching $\geq$60% more than 24 hours after irradiation. Damage to cells was great (Fig. 3).

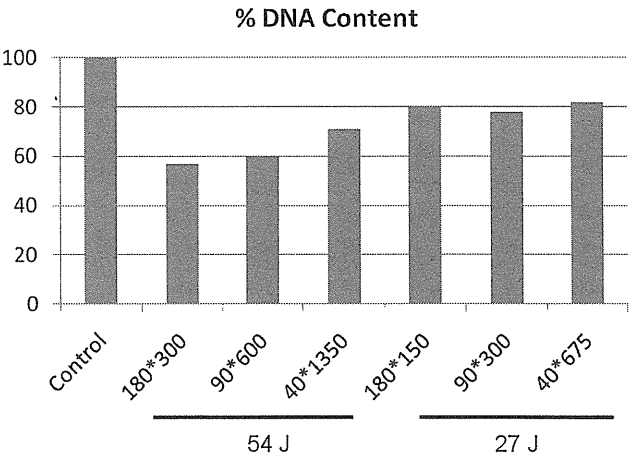


Fig. 2. Use of %DNA content as a marker of surviving cells after laser irradiation. In the 54-J total energy group ($n = 8$), %DNA content was 60–70%, and tended to decrease as the amount of energy per shot increased. In the 27-J group ($n = 8$), in contrast, %DNA content was about 80% in all cases. (e.g., 180 × 300: 180 mJ/pulse × 300 shots = total 54 J).

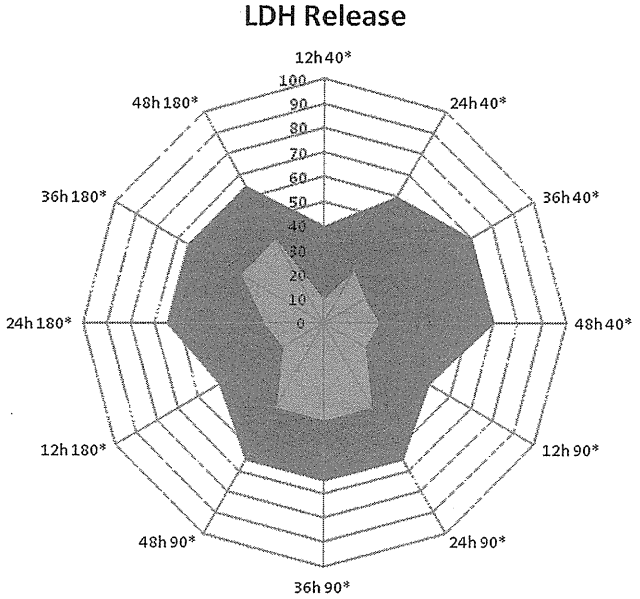


Fig. 3. LDH release as a marker of cell membrane damage. In the total energy 27-J group ($n = 8$), LDH release was 10–35% and the injury to cells was mild. In the 54-J group ($n = 8$), values were ≥40% from 12 hours after irradiation and reached ≥60% more than 24 hours after irradiation. The damage to cells was great. Red area: Groups of 54 J, Blue area: Groups of 27 J, (ex; 12 hours 40*; 40 mJ/pulse ×675 or 1,350 shots = total 27 J or 57 J irradiation after 12 hours).

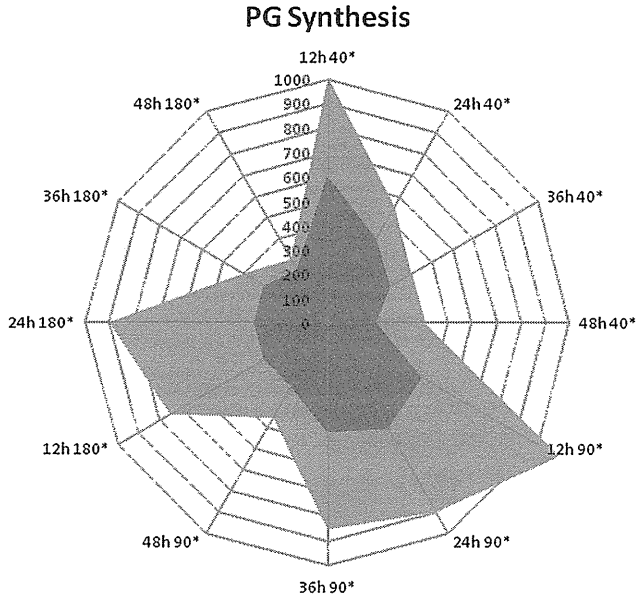


Fig. 4. Proteoglycan synthesis as a marker of synthesis of extracellular matrix. Proteoglycan synthesis was low overall in the 54-J group ($n = 8$), and synthesis was inhibited by the high level of cell damage. In the 27-J group ($n = 8$), in contrast, some cases showed high synthetic activity depending on the irradiation conditions. Red area: Groups of 54 J, Blue area: Groups of 27 J, (ex; 12 hours 40*; 40 mJ/pulse ×675 or 1,350 shots = total 27 J or 57 J irradiation after 12 hours).

### Matrix Synthetic Capacity

Proteoglycan synthesis was low overall in the 54-J group, and synthesis was inhibited by the high level of cell damage. In the 27-J group, in contrast, cases of high synthetic activity were seen, depending on the irradiation conditions (Fig. 4). Matrix-synthesizing capacity at 12 hours after irradiation was large, and cell activity was thought to be modified considerably. In the 90-mJ/pulse condition in particular, activation of proteoglycan synthesis was maintained a long time after irradiation compared with other conditions.

### Influence of Photoacoustic Effect

Figure 5 shows the relationship between the photoacoustic effect and LDH release and proteoglycan synthesis. Linear correlations were obtained in both the 27- and 54-J groups, and this experiment clarified the influence of the photoacoustic effect on cells. Proteoglycan synthesis in particular was thought to be susceptible to influences from the photoacoustic effect.

### Influence of Photothermal Effect

Figure 6 shows the relationship between the photothermal effect and LDH release and proteoglycan synthesis. A weak linear correlation with LDH release was seen in the 54-J group, but no other correlations were seen in either the 27- or 54-J groups.

## DISCUSSION

We have previously focused on the fact that the cells contained in intervertebral discs form a chondron-like morphology in tissue similar to articular cartilage, and confirmed that the biological status of these cells in the body could be reproduced in three-dimensional culture [21–23]. Then, by three-dimensional culture of the component cells of intervertebral discs, as an aggregate of heterogenous cells from the inner and outer layers of the intervertebral disc, a homogenous cytoplasm was obtained. The essentially different features of the inner and outer layers of the annulus fibrosus were confirmed to have been eliminated [21]. In other words, the uniform cell populations created by three-dimensional culture could be used to evaluate cell damage and matrix synthesis of cells in an environment similar to that of tissue. With the use of this three-dimensional model, complex cell reactions in the body resulting from laser irradiation can be evaluated *in vitro*.

From the results for DNA content and LDH release, damage to cells appeared mild in the 27-J group. However, findings suggested that in the 54-J group, necrosis occurs over a wide range out from the center in the early phase after irradiation. With proteoglycan synthesis, some cases showed maintenance of high synthetic activity over a long period depending on the irradiation conditions in the 27-J group. This indicates that with appropriate

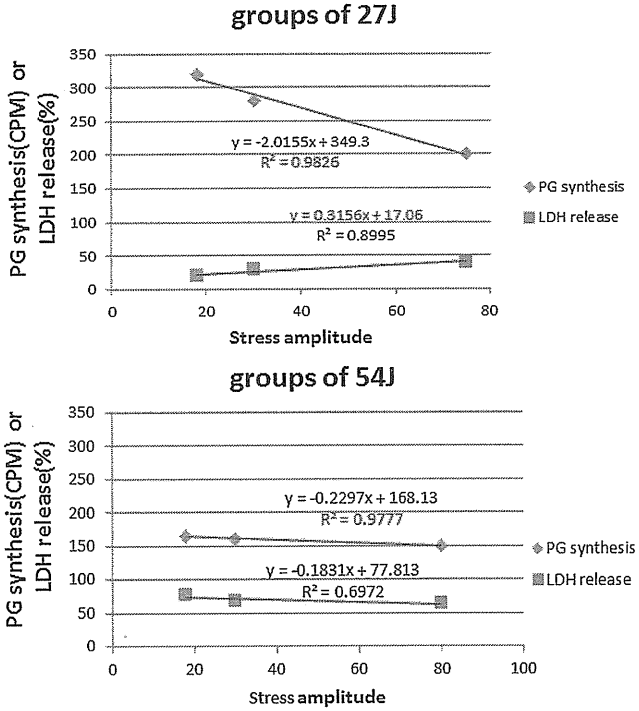


Fig. 5. Correlation between PG synthesis/LDH release and stress amplitude. Linear correlations were obtained in both the 27- and 54-J groups ($n$ = 8 each). Proteoglycan synthesis in particular was considered susceptible to influences from the photoacoustic effect. Tests were performed at three different stress amplitudes.

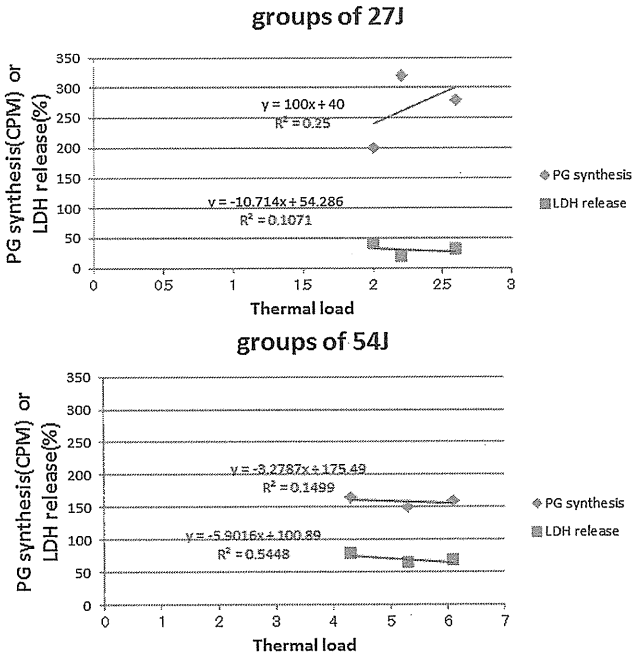


Fig. 6. Correlation between PG synthesis/LDH release and thermal load. A weak linear correlation with LDH release was seen in the 54-J group ($n$ = 8), but no other correlations were found. Tests were performed in each group at three different thermal loads.

irradiation conditions, intervertebral disc cells are activated without causing total cell death, and local matrix synthesis flourishes, suggesting that this is a condition in which decreased pressure is obtained from tissue vaporization of the irradiation site with laser irradiation, while at the same time increasing the reparative abilities of the tissue around the irradiation site. Tissue damage from PLDD may thus be able to be minimized. This kind of cell activation effect does not exist in conventional percutaneous nucleotomy, in which the nucleus pulposus is extracted using a punch, and is thought to be a characteristic effect of laser irradiation. In an actual clinical situation, we believe that laser irradiation should not performed continuously from beginning to end. It should be performed in intervals; tissue-cooling time should be set; and laser irradiation should be broken up several times. Local heat retention needs to be monitored in a timely manner, but no medical devices currently enable detailed and appropriate monitoring of the laser irradiation tip. We look forward to the development of medical devices that enable monitoring of local status to provide clinical feedback on irradiation conditions, so that one of the characteristic effects of lasers, the elevation of proteoglycan synthesis, can be fully displayed.

A threshold level is known to exist in the thermal load. With 54 J, LDH release reaches ≥60% and proteoglycan synthesis is also low, suggesting that extensive damage occurs in many cells within environments that are already above the threshold. However, to understand the thermal load in greater detail, more refined methods will be necessary with closer monitoring, not just in the high range above a certain standard temperature (≥50°C in this study).

Laser irradiation produces both photothermal and photoacoustic effects, but the impact on cells is conjectured to differ depending on the total energy. Total energy is closely related to optimization of irradiation conditions, and irradiation conditions in the 27-J group are beneficial from the perspectives of a cytoprotective effect and promotion of matrix synthesis, and may be conditions that can be extrapolated to clinical practice. Evaluation methods in this study that enabled *in vitro* measurement and evaluation of cell reactions caused by both photothermal and photoacoustic effects from laser irradiation may be useful in optimizing laser irradiation conditions.

In conclusion, the three-dimensional culture model of intervertebral disc cells is excellent for clarifying the relationship between cell reactions, photoacoustic effect, and photothermal effect resulting from laser irradiation. In addition, total energy is closely related to optimization of irradiation conditions, and irradiation conditions in the 27-J group were beneficial from the perspectives of cytoprotection and promotion of matrix synthesis, and may be conditions that can be extrapolated to clinical practice.

## ACKNOWLEDGMENTS

The authors thank Prof. Tsunenori Arai, Department of Applied Physics and Physico-Informatics, Faculty of Science and Technology, Keio University, Japan for providing useful information, comments, and technical critique with Ho:YAG laser irradiation.

## REFERENCES

1. Choy DS, Case RB, Fielding W, Hughes J, Liebler W, Ascher P. Percutaneous laser nucleolysis of lumbar disks [letter]. N Engl J Med 1987;317:771–772.
2. Choy DS, Ascher PW, Ranu HS, Saddeknis S, Alkaitis D, Liebler W, Hughes J, Diwan S, Altman P. Percutaneous laser disc decompression. A new therapeutic modality [published erratum appears in Spine 1993; Jun 1;18(7):939]. Spine 1992;17:949–956.
3. Yonezawa T, Onomura T, Kosaka R, Miyaji Y, Tanaka S, Watanabe H, Abe Y, Imachi K, Atumi K, Chinzei T, Mabuchi K, Fujimasa I. The system and procedures of percutaneous intradiscal laser nucleotomy. Spine 1990;15:1175–1185.
4. Davis JK. Percutaneous discectomy improved with KTP laser. Clin Laser Mon 1990;8:105–106.
5. Gottlob C, KopcHok GE, Peng SK, Tabbara M, Cavaye D, White RA. Holmium:YAG laser ablation of human intervertebral disc: Preliminary evaluation. Lasers Surg Med 1992; 12:86–91.
6. Quigley MR, Shih T, Elrifai A, Maroon JC, Lesiecki ML. Percutaneous laser discectomy with the Ho:YAG laser. Lasers Surg Med 1992;12:621–624.
7. Sato M,Ishihara M,Arai T, et al. Use of a new ICG-dye-enhanced diode laser for percutaneous laser disc decompression. Lasers Surg Med 2001;29:282–287.
8. Niemz MH. Laser-Tissue Interactions Fundamentals and Applications (Third, Revised Edition). Biological and Medical Physics, Biomedical Engineering. Springer. 2004; XVI: 65.
9. Arai T. A review for new laser devices for laser therapy in gastroenterology. J Jpn Soc Laser Surg Med 1993;14:13–20.
10. Yoshikawa M, Nakajima A, Arai T, Kikuchi M, Kannari H, Obara M. The measurement of cavity collapse time by probe technique on water, agar, and vascular tissue during Ho:YAG laser contact ablation. Proc SPIE 1993;1882:382–387.
11. Tonami H, Kuginuki M, Kuginuki Y, et al. MR imaging of subchondral osteonecrosis of the vertebral body after percutaneous laser diskectomy. Am J Roentgenol 1999;173:1383–1386.
12. Uto Y, Mochida J, Nomura T. The clinical case study of postoperative condition on Percutaneous Laser Disc Decompression. Kanto J Orthop Traumatol 2003;34: 27–31.
13. Takeno K, Kobayashi S, Yonezawa T, Hayakawa K, Hachiya Y, Uchida K, Negoro K, Timbihurira G, Baba H. Salvage operation for persistent low back pain and sciatica induced by percutaneous laser disc decompression performed at outside institution: Correlation of magnetic resonance imaging and intraoperative and pathological findings. Photomed Laser Surg 2006;24:414–423.
14. Sato M, Ishihara M, Arai T, Asazuma T, Kikuchi T, Kikuchi M, Fujikawa K. Study for the optimum Ho:YAG laser irradiation condition on the percutaneous laser disc decompression (PLDD): In vitro quantitative evaluation of the influence on disc cells using three-dimensional cell culture system. Proc SPIE 1999;3601:387–391.
15. Sato M, Ishihara M, Arai T, Asazuma T, Kikuchi T, Kikuchi M, Fujikawa K. Study for the Ho:YAG laser—Intervertebral disc cell interaction using three-dimensional cell culture system. Proc SPIE 2000;3914:216–221.
16. Srinivasan R, Dyer PE, Braren B. Far-ultraviolet laser ablation of the cornea: Photoacoustic studies. Lasers Surg Med 1987;6(6) 514–519.
17. Kim YJ, Sah RL, Doong JY, Grodzinsky AJ. Fluorometric assay of DNA in cartilage explants using Hoechst 33258. Anal Biochem 1988;174:168–176.
18. de Luca A, Weller M, Fontana A. TGF-beta-induced apoptosis of cerebellar granule neurons is prevented by depolarization. J Neurosci 1996;16:4174–4185.
19. Dimmeler S, Haendeler J, Nehls M, Zeiher AM. Suppression of apoptosis by nitric oxide via inhibition of interleukin-1beta-converting enzyme (ICE)-like and cysteine protease protein (CPP)-32-like proteases. J Exp Med 1997;185:601–607.
20. Masuda K, Shirota H, THonar EJ. Quantification of 35S-labeled proteoglycans complexed to alcian blue by rapid filtration in multiwell plates. Anal Biochem 1994;217:167–175.
21. Sato M, Kikuchi T, Asazumz T, Yamada H, Maeda H, Fujikawa K. Glycosaminoglycan accumulation inprimary culture of rabbit intervertebral disc cells. Spine 2001;26:2653–2660.
22. Sato M, Asazuma T, Ishihara M, Kikuchi T, Masauoka K, Ichimura S, Kikuchi M, Kurita A, Fujikawa K. An atelocollagen Honeycomb-shaped scaffold with a membrane seal (ACHMS-scaffold) for the culture of annulus fibrosus cells from an intervertebral disc. J Biomed Mater Res 2003;64A: 248–256.
23. Sato M, Yamamoto Y, Sakai D, Mochida J. Characterization of intervertebral disc–disc cells and pericellular microenvironment. Clin calcium 2004;14:64–69.

整・災外 54：839—843，2011

新しい医療技術

# ナノ秒パルスレーザーによる鏡視下関節軟骨の機能評価

佐藤正人[*1)] 石原美弥[*2)] 三谷玄弥[*1)]
沓名寿治[*1)] 菊地眞[*2)] 持田譲治[*1)]

**要旨**：関節軟骨本来の機能に基づく客観的評価方法が臨床の現場で欠如している。軟骨変性の進行は緩徐であり，評価方法のエンドポイントの設定も難しい。関節疾患の保存療法または術後評価は，患者の自覚症状やX線像での関節裂隙の狭小化の程度から推察しているに過ぎず，関節軟骨本来の機能に基づく客観的指標がないことで臨床評価が曖昧になることは，大きな問題である。関節軟骨本来の機能である力学特性（粘性，弾性，潤滑）と組織性状を正確に計測し，定量的に評価することが，より詳細な病態把握と治療効果判定に重要である。われわれは，定量的な関節軟骨機能の臨床診断法の確立を目指して，光音響原理に基づく力学特性評価と，時間分解自家蛍光スペクトル分析による組織性状評価の有効性を確認した。今後データを集積できれば，多角的に変形性関節症の詳細な病態把握が可能となり，患者に対して，よりきめ細かな治療計画の立案と遂行が可能となり，高齢者の健康寿命延伸に寄与するものと考える。

## はじめに

関節疾患は，生命を直接脅かすものではないが，要支援となる原因疾患の第1位であり，ADLを下げるばかりかQOLの低下も招き，人的・社会的損失は計り知れない。低侵襲に関節軟骨本来の機能である力学特性と組織性状を正確に計測し，定量的に評価することができれば，変形性膝関節症をはじめとする軟骨変性を伴う運動器疾患の正確な病態把握と治療計画，ならびにその遂行が可能となるばかりか，新薬等の治験の際の客観的評価法としても有用と考えている。そして，臨床データの蓄積により，詳細な病態把握と予後診断が可能となり，個々の患者の病態に応じた，きめ細かな治療計画も可能となる。

本評価法は，平成17年度からの5カ年のNEDO事業「健康安心イノベーションプログラム/再生医療の早期実用化を目指した再生評価技術開発」で培った再生軟骨（組織工学的軟骨）の*in vitro*の非侵襲評価技術を発展させたものである。平成19年度から3カ年の厚労省科学研究費補助金（長寿科学総合事業）で継承し，世界で初めて実証した光音響原理に基づく力学特性評価と，時間分解自家蛍光スペクトル分析による組織性状評価による，関節軟骨機能の臨床診断技術の開発を目指したものである。

本研究で用いる計測技術は，“日本発・世界初”

*1) Masato SATO et al，東海大学医学部，外科学系整形外科学
*2) Miya ISHIHARA et al，防衛医科大学校，医用工学

Evaluation of articular cartilage using nanosecond pulsed laser under arthroscopy

**Key words**：Articular cartilage evaluation, Nanosecond pulsed laser, Arthroscopy

のもので，光音響原理に基づく粘弾性計測法の原理を提案し，検証実験でその有用性を確認したものである[1]。光音響信号を効率的に励起できる波長330 nmのパルスレーザーを使用することで，薬剤等の修飾なく測定可能な自家蛍光波長と時間を関数とした分析も可能となり，力学特性[2)~15)]と組織性状[16)~27)]とを同時に定量的に計測することが可能な技術を開発した[17]。本計測技術は当初，組織工学的に作製した再生軟骨の移植前の *in vitro* 評価法として確立した[3)~6)]。しかし，実際の臨床で，関節軟骨の診断において使用しなければならないのは，関節鏡視下環境であることが多い。

本研究においては，この評価技術を関節鏡視下で実施可能なレベルまでスケールダウンすることから始まった。つまり，励起用レーザー光の導光系と光音響信号と自家蛍光の検出センサーを一体化し，関節内計測用の曲げプローブを開発し，さらに，測定プロトコールの最適化によりハイスループットな計測を目指した。これらの実現により，臨床へのアプリケーションは大いに拡大された。すなわち，再生医療の評価技術として用いるばかりでなく，高齢者の多くに認められる軟骨変性の診断のために，関節軟骨本来の力学特性と組織性状とに基づく，関節鏡視下で定量評価可能な新規の軟骨機能診断法として，疾患病態の解明と治療効果判定に威力を発揮するものと考えた。

## Ⅰ．原理と方法

光やレーザー光を計測対象である生体へ照射する結果として，散乱，反射，ならびに吸収に伴う温度上昇，さらには蛍光や音響波発生等が主な作用として挙げられる。最近注目されている光を利用した経ファイバー的，非侵襲的，選択的な診断補助装置は，このようなレーザー光と生体との相互作用の特長を生かした技術に立脚している[17]。本評価法で使用している軟骨の粘弾性計測のための光音響法は応力波発生という現象を利用したphotoacousticな作用を利用したものであり，一方，軟骨の性状評価のための自家蛍光スペクトル解析は蛍光発生という現象を利用したphotochemicalな作用を利用したものである[23)26)27)]。同一のレーザーが生体との間で異なる相互作用を生じるため，これらの相互作用を利用することで，形態情報だけでなく，生理的，生化学的な多くの情報をも同時取得することが可能であることから，超音波のような単一情報の解析よりも，診断装置としての将来性が大いに見込まれている。

われわれは，関節軟骨の本来の機能特性である力学特性と組織性状を，ナノ秒パルスレーザー照射することにより，非侵襲的に得られる光音響信号と蛍光情報から評価する技術を開発し，関節鏡視下に適用可能とし，変形性関節症など軟骨変性を伴う慢性関節炎等の正確な病態把握と各種治療による効果判定の定量評価を可能とするシステムを開発することを考えた[18]。そのために，光音響法と時間分解スペクトル分析法に必要不可欠な各要素技術を臨床使用可能なレベルに押し上げ，さらに，プロトタイプ装置，プローブ，解析ソフトの開発，改良を行い，実際の臨床の現場での術者の使用感もフィードバックするようにした。

## Ⅱ．研究結果

### 1．光音響法による力学特性評価法

レーザー照射により，局所で発生した応力波が組織内を伝播する過程で組織固有の粘弾性により減衰する現象に着目し，光音響法で力学特性を計測できる基本原理を提案した。研究開発当初はレーザー光の至適な波長が不明であったため，コラーゲンやタンパクを光の吸収体として考慮し，実用性を考慮すると，小型，可搬，安価な励起光源が望まれるため，Qスイッチ Nd：YAG レーザーの第3高調波（波長：355 nm，パルス幅：5～6ns）を使用したシステムとした[2)~4)]。出力光は石英光ファイバー（コア径：400 nm）で導光し，光音響波の検出には，圧電性高分子フィルムのポリフッ化ポリビニリデン共重合体〔P(VdF/TrFE)〕を用いたプローブを開発した。これは，光ファイバーをプローブの中央に配置して，センサーをその周囲にリング状に配置して一体化した反射型プローブであり関節鏡視下でも計測可能なものである。

## 2．時間分解自家蛍光スペクトル解析による組織性状評価法

時間分解自家蛍光計測（TR-LIFS）においても，光音響法と同様に，励起光は光ファイバーで導光したQスイッチNd：YAGレーザー第3高調波を用い，ナノ秒オーダーのゲートで測定可能な分光システムを4チャンネルのデジタルパルスジェネレータで制御しながら施行した[16)~25)]。計測パラメータは，蛍光ピーク強度，半値幅，ピーク波長，蛍光体積，蛍光寿命を算出した。関節軟骨は，Ⅱ型コラーゲンに近似したスペクトルを呈し，ピーク波長ならびに半値幅も近似した。一方，椎間板線維輪外層はⅠ型コラーゲンに近似したスペクトルを呈し，同様にピーク波長ならびに半値幅も近似した[16)17)]。これらの結果は，生体内の自家蛍光物質であるコラーゲンの組成までも，非接触で計測可能であることを示したものであり，特に軟骨の変性度の診断に関してはⅠ型，Ⅱ型コラーゲンの含有比は重要と考えられており，これらを非侵襲的に計測可能な技術開発は軟骨評価法として意義深い。

## 3．臨床応用

本研究事業で開発した技術を用いて，東海大学医学部付属病院で関節鏡手術の際に臨床応用を施行している。細径化したプローブを用いて，関節鏡の術中のモニター表示画面の一部に計測波形をリアルタイムにモニター表示して術者が計測を実感できるように工夫した。この波形表示の仕方は，モニター中に大きくも小さくも可能である（図1）。

本計測法は，関節鏡視下の水中でも，関節を切開したオープンサージェリー，すなわち空気中でも実施可能である。粘弾性計測と同時に，関節軟骨の厚さも計測しているが，その際に音速で近似しているため，その部分で水中と空気中で，わずかな誤差が生じるが臨床で扱う計測結果としては問題とならない。

以下に臨床症例の計測結果表示例を提示する（図2）。関節鏡視下所見をOuterbridge classificationで，軟骨損傷程度をICRS分類で示したが，計測した光音響法での波形と軟骨の厚さ，および時間分解自家蛍光スペクトルを提示する。軟骨変性が進むとともに応力緩和時間$\tau$は延長し，粘性が大きくなる傾向にあった。また軟骨の厚さも変性とともに減少し，自家蛍光スペクトルはシャープなものからややブロードな二峰性を呈するようになった。

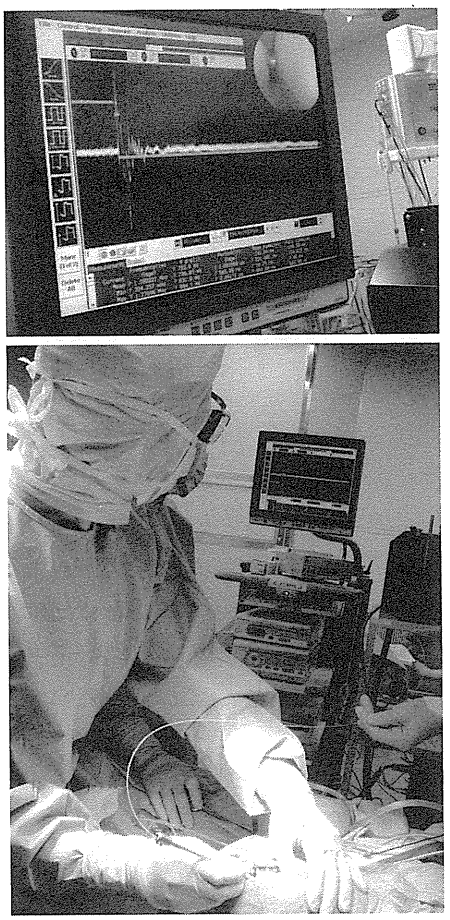

図1　手術時の計測状況

## Ⅲ．考　察

本評価法は，関節鏡視下環境を必要とするが，粘弾性特性，性状評価，軟骨の厚さや表面構造の評価なども定量化でき，軟骨の評価に有用な情報を一気に得られる点が特に優れていると考えられる。光は選択するレーザーの波長や種類で非常に守備範囲の広いモダリティであり，そのため各種のモダリティとの併用あるいは融合が可能である。それによって，さらに正確な軟骨の診断が可能になると期待している。つまり，関節全体を描

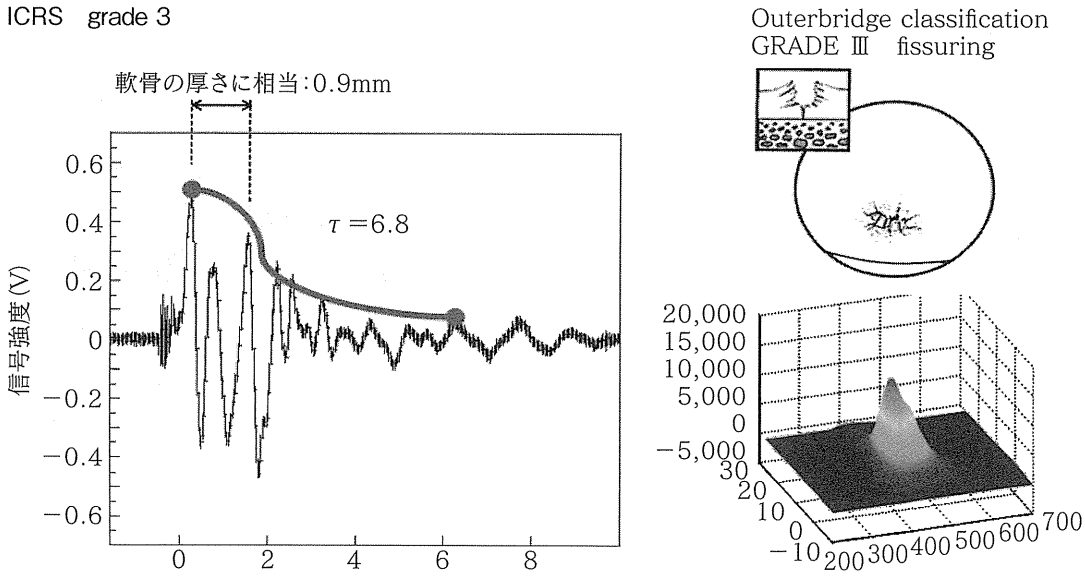


**図 2** 鏡視下軟骨計測の結果

出できるような画像構築に優れたモダリティと組み合わせれば,軟骨の変性度やその広がり具合も,画像とともに定量的に評価でき,変形性関節症のstructure modifying effectが評価可能となり,初めて適正な治療効果の判定が可能となるのではないかと考えている。

われわれは,本研究事業を通して,非侵襲的な微弱なパルスレーザーを用いて,関節鏡視下に関節軟骨の力学特性と性状評価を同時に施行可能であることを示した。そして,現在その標準化と実用化に向けて,試行錯誤を繰り返しながら取り組んでいる。本評価技術が実用化され,関節鏡視下で関節軟骨本来の機能である力学特性と組織性状を,整形外科医が正確に定量的に機能評価することが可能となれば,変形性関節症の正確な病態把握が可能となり,病態,病期ごとのきめ細かな治療法が確立し,根治の可能性が見えてくるのではないかとわれわれは考えている。さらに,各種の薬剤等の治療効果に関しても,従来の関節周囲の痛みやADL障害といった自覚症状に基づくものや炎症症状といった臨床症状の評価に加え,定量的に関節軟骨の力学特性と組織性状とを同時に計測し評価する本技術は,新薬等の治験の際の客観的評価法としても極めて有用と考えられる。つまり,従来エンドポイントが不明瞭な変形性関節症に対して,関節軟骨の変性の進行度(病期)を定量的に評価することで,構造修飾効果を客観的に評価し得るものと考える。また,各種モダリティ(特に画像診断装置)との組み合わせにより,本計測技術はさらに効果を発揮していくものと考える。

## おわりに

関節鏡視下での観察や治療の際に,本計測により力学的評価と組織性状評価のデータが同時に多角的かつ定量的に今後集積されれば,軟骨変性診断の細分化が進み,そのgradeから各種の治療効果や予防対策などが明らかになるものと考える。

## 文　献

1) Ishihara M et al：Viscoelastic characterization of biological tissue by photoacoustic measurement. Jpn J Appl Phys **42**：556—558, 2003
2) Ishihara M et al：Development of a photoacoustic measurement method for the evaluation of regenerative medicine and tissue engineering for articular cartilage. J Jpn Soc Laser Surg Med **26**：53—59, 2005
3) Ishihara M et al：Usefulness of the photoacoustic measurement method for monitoring the

regenerative process of full-thickness defects in articular cartilage using tissue-engineering technology. Proc SPIE **5695**：288—291, 2005
4) Ishihara M et al：Usefulness of photoacoustic measurements for evaluation of biomechanical properties of tissue-engineered cartilage. Tissue Eng **11**：1234—1243, 2005
5) Ishihara M et al：Development of a noninvasive multifunctional measurement method using nanosecond pulsed laser for evaluation of regenerative medicine for articular cartilage. Proc SPIE **6084**：60840 V. 1—60840 V. 4, 2006
6) Ishihara M et al：Development of a diagnostic system for osteoarthritis using a photoacoustic measurement method. Lasers Surg Med **38**：249—255, 2006
7) 石原美弥ほか：再生医療評価・バリデーションのための非侵襲的計測法．生物工学会誌 **85**：438—441, 2007
8) 菊地　眞ほか：再生医療の基盤技術としての計測・画像工学．再生医療のためのバイオエンジニアリング，コロナ社，147—167, 2007
9) 石原美弥ほか:バイオメディカルイメージング．再生医療技術の最前線，シーエムシー出版，61—68, 2007
10) 石原美弥ほか:レーザーを用いた培養軟骨評価．再生医療に用いられる細胞・再生組織の評価と安全性，シーエムシー出版，123—137, 2007
11) Ishihara M et al：Multifunctional evaluation of tissue engineered cartilage using nano-pulsed light for validation of regenerative. IFMBE Proceedings WC **14**：3187—3189, 2007
12) 石原美弥ほか：ナノ秒パルスレーザーによる細胞外マトリックスの構築モニター．電気学会論文誌 **127-C**：2166—2170, 2007
13) Ishihara M et al：Usefulness and limitation of measurement methods for evaluation of tissue-engineered cartilage function and characterization using nanosecond pulsed laser. Proc SPIE **6439**：643909.1—643909.4, 2007
14) Ishihara M et al：Modification of measurement methods for evaluation of tissue engineered cartilage function and biochemical properties using nanosecond pulsed laser. Proc SPIE **6558**：685805.1—685805.5, 2008
15) Sato M et al：Recent technological advancements related to articular cartilage regeneration. Med Biol Eng Comput **46**：735—743, 2008
16) Ishihara M et al：Modification of measurement methods for evaluation of tissue-engineered cartilage function and biochemical properties using nanosecond pulsed laser. Proc SPIE **6858**：685804.1—685804.5, 2008
17) 佐藤正人ほか：変形性関節症の病態把握と治療効果判定を可能にする定量的機能診断システムの開発ーナノ秒パルスレーザーを用いた力学特性と組織性状の同時計測を目指して．別冊整形外科 No. 53：76—82, 2008
18) Ishihara M et al：Modification of measurement methods for evaluation of tissue engineered cartilage function and biochemical properties using nanosecond pulsed laser. Proc SPIE **6858**：685804.1—685804.6, 2008
19) 石原美弥ほか：再生医療を光で評価する．第4回集積光デバイス技術時限専門委員会誌 **IPD08**：44—49, 2008
20) Sato M et al：Recent technological advancements related to articular cartilage regeneration. Med Biol Eng Comput **46**：735—743, 2008
21) 石原美弥ほか：光による再生医療に用いる組織・細胞の評価．Microoptics News **26**：31—36, 2008
22) 石原美弥ほか：高齢者の ADL（Activity of Daily Life）維持に貢献する変形性関節症の早期診断システムの研究開発．未病と抗老 **18**：110—114, 2009
23) Kutsuna T et al：Noninvasive evaluation of tissue engineered cartilage with time-resolved laser-induced fluorescence spectroscopy. Tissue Eng Part C Methods **16**：365—373, 2009
24) Ishihara M et al：Multifunctional characterization of engineered cartilage using nano-pulsed laser. IFMBE Proc **25**：69—70, 2009
25) 石原美弥ほか：軟骨再生医療に有効な光技術．整・災外 **52**：1533—1537, 2009
26) Sato M et al：Development of a diagnostic system for osteoarthritis using a photoacoustic measurement method and tome-resolved autofluorescence. Bioengineering；Principles, Methodologies and Applications, Nova Science Publishers, 2010
27) Sato M et al：A diagnostic system for articular cartilage using non-destructive pulsed laser irradiation. Lasers Surg Med（in press）

Lasers in Surgery and Medicine 43:421–432 (2011)

# A Diagnostic System for Articular Cartilage Using Non-Destructive Pulsed Laser Irradiation

**Masato Sato, MD, PhD,[1]* Miya Ishihara, PhD,[2] Makoto Kikuchi, PhD,[2] and Joji Mochida, MD, PhD[1]**
[1]*Department of Orthopaedic Surgery, Surgical Science, Tokai University School of Medicine, 143 Shimokasuya, Isehara, Kanagawa 259-1193, Japan*
[2]*Department of Medical Engineering, National Defense Medical College, 3-2 Namiki, Tokorozawa, Saitama 359-8513, Japan*

**Background and Objectives:** Osteoarthritis involves dysfunction caused by cartilage degeneration, but objective evaluation methodologies based on the original function of the articular cartilage remain unavailable. Evaluations for osteoarthritis are mostly based simply on patient symptoms or the degree of joint space narrowing on X-ray images. Accurate measurement and quantitative evaluation of the mechanical characteristics of the cartilage is important, and the tissue properties of the original articular cartilage must be clarified to understand the pathological condition in detail and to correctly judge the efficacy of treatment. We have developed new methods to measure some essential properties of cartilage: a photoacoustic measurement method; and time-resolved fluorescence spectroscopy.

**Materials and Methods:** A nanosecond-pulsed laser, which is completely non-destructive, is focused onto the target cartilage and induces a photoacoustic wave that will propagate with attenuation and is affected by the viscoelasticity of the surrounding cartilage. We also investigated whether pulsed laser irradiation and the measurement of excited autofluorescence allow real-time, non-invasive evaluation of tissue characteristics.

**Results:** The decay time, during which the amplitude of the photoacoustic wave is reduced by a factor of $1/e$, represents the key numerical value used to characterize and evaluate the viscoelasticity and rheological behavior of the cartilage. Our findings show that time-resolved laser-induced autofluorescence spectroscopy (TR-LIFS) is useful for evaluating tissue-engineered cartilage.

**Conclusions:** Photoacoustic measurement and TR-LIFS, predicated on the interactions between optics and living organs, is a suitable methodology for diagnosis during arthroscopy, allowing quantitative and multidirectional evaluation of the original function of the cartilage based on a variety of parameters. Lasers Surg. Med. 43:421–432, 2011. © 2011 Wiley-Liss, Inc.

**Key words:** osteoarthritis; photoacoustic measurement; time-resolved autofluorescence spectroscopy; tissue-engineered cartilage



## INTRODUCTION

Osteoarthritis is thought to affect about 30 million people in Japan [1], but is not a direct threat to life. However, this condition both affects activities of daily living and diminishes quality of life among sufferers, so the associated human and social loss is difficult to estimate. The disease involves dysfunction caused by cartilage degeneration, but objective methodologies of evaluation based on the original function of the articular cartilage are currently unavailable. Evaluations that are currently used to establish conservative therapies or the prognosis of surgery as a treatment for osteoarthritis are merely based on patient symptoms or the degree of joint space narrowing on X-ray images. Accurate measurement and quantitative evaluation of the mechanical characteristics of cartilage (viscosity, elasticity, and lubrication) are important, and the tissue properties of the original articular cartilage need to be recognized if the pathological condition is to be understood in detail and treatment effects judged accurately. The development of such evaluation technologies is thus required to facilitate a functional diagnosis of osteoarthritis. If these evaluations can be achieved non-invasively, an accurate understanding of the pathologies should be possible, allowing the planning and performance of treatments for locomotor apparatus diseases that accompany the degeneration of cartilage, such as osteoarthritis. Such evaluations would also be useful as objective tools in situations such as the clinical

Conflict of interest statement: None.
Contract grant sponsor: Takeda Science Foundation; Contract grant sponsor: General Insurance Association of Japan; Contract grant sponsor: Mitsui Sumitomo Insurance Welfare Foundation; Contract grant sponsor: High-Tech Research Centre Project for Private Universities; Contract grant sponsor: Ministry of Education, Culture, Sports, Science, and Technology of Japan; Contract grant sponsor: New Energy and Industrial Technology Development Organization; Contract grant sponsor: Japan Foundation for Aging and Health.
*Corresponding to: Dr. Masato Sato, MD, PhD, Department of Orthopaedic Surgery, Surgical Science, Tokai University School of Medicine, 143 Shimokasuya, Isehara, Kanagawa 259-1193, Japan. E-mail: sato-m@is.icc.u-tokai.ac.jp
Accepted 28 March 2011
Published online 15 June 2011 in Wiley Online Library (wileyonlinelibrary.com).
DOI 10.1002/lsm.21065

trials of new drugs. A better understanding of the pathological condition in detail and determination of prognosis based on a body of clinical data should thus be possible. This will in turn facilitate the careful planning of treatments according to the specific pathological conditions of individual patients, improving activities of daily living, and enhancing the lives of many people.

Recent studies have suggested ultrasonography (US) as a sensitive method for determining cartilage thickness [2,3], structural properties [4], surface roughness [5], and enzymatically induced, specific degeneration of the superficial collagen network [6–8]. Mechanically, the collagen network is primarily responsible for the dynamic properties of cartilage by constraining transversal expansion, whereas proteoglycans contribute predominantly to interstitial fluid flow and the equilibrium response of cartilage [9,10]. Structural and mechanical properties vary within and between different articular surfaces [11,12]. Hattori et al. [13,14], reported a method to assess joint cartilage using US. By limiting examination to the mechanical properties of joint surfaces, cartilage can be assessed by indentation testing [15–17]. For the clinical diagnosis of mechanical properties, as with indentation testing, US requires arthroscopy. Quantitative intra-articular US imaging [18–20] and Optical coherence tomography [21,22] have been already been applied in vivo during knee surgery. MRI excels at geographical mapping, and while one advantage is the ability to gather a wide variety of extra-articular data, unlike US or indentation testing, viscoelastic properties cannot be directly measured. Normal and abnormal signals on images are simply compared to indirectly estimate mechanical properties. Several quantitative MRI techniques have recently been introduced for the non-invasive assessment of structural and mechanical properties of articular cartilage [23]. T2 mapping is sensitive to the integrity of collagen networks, collagen content, and fibril orientation [24–26]. T1 mapping in the presence of Gd-DTPA2 contrast agent, namely delayed gadolinium-enhanced MRI of cartilage (dGEMRIC), reflects the proteoglycan distribution in cartilage via the inverse distribution of ionic contrast agent [27,28].

The method of assessing cartilage function using a non-invasive pulsed laser that we have been analyzing is a technique focusing on interactions with the body when the laser is applied to cartilage. In other words, this photoacoustic method is a technique for measuring viscoelastic properties based on how sound waves travel and attenuate through the body and resembles US. Time-resolved laser-induced autofluorescence spectroscopy (TR-LIFS) measures autofluorescence generated through other interactions, and analyzes the properties of characteristically collagen-rich cartilage tissue matrix using the same laser irradiation. In other words, with our proposed method employing pulsed laser irradiation, interactions are measured by two different methods to obtain more biological information than US or indentation testing (Table 1). Relaxation times as measured by the photoacoustic method agreed well with the intrinsic viscoelastic parameters, with a correlation coefficient of 0.98, when

**TABLE 1. Comparison of Major Cartilage Measurement Devices**

| | Indenter | Ultrasound | Laser (LIPA + TR-LIFS) | MRI |
|---|---|---|---|---|
| Direct measurement of viscoelasticity properties | Possible (up to superficial layer) large impacts of force application and superficial layer | Possible (average from surface to deep layers) | Possible (average from surface to deep layers) | Unable |
| Assessment of surface structures (fibrillation, etc.) | Possible | Possible | Possible | Unable |
| Compostional information (collagen content) | Unable | Possible (imaging) | Possible (distinguishable COL1 and COL2) | Possible (imaging) |
| Arthroscopic environment | Necessary | Necessary | Necessary | Unnecessary |

LIPA, laser-induced photoacoustic measurement; TR-LIFS, time-resolved laser-induced autofluorescence spectroscopy; COL1, collagen type 1; COL2, collagen type 2. Viscoelasticity can be measured directly using an indenter, ultrasound system, or laser. However, these devices all require arthroscopy. Conversely, MRI excels at geographical mapping and is advantageous for gathering a wide variety of extra-articular information, but the mechanical properties of abnormal signals can only be estimated indirectly based strictly on image changes, and delineating fine joint surface structures is difficult. Using a laser, COL1 can be differentiated from COL2. This method is thus suited for assessing tissue properties.